'93 KACC (1993.10.20~22)

4 Degrees of Freedom Control for a Magnetically Levitated Vehicle

KookHun Kim, ChoonKyung Kim, JongMoon Kim, ChangHee Cho, MinKook Park
Korea Electrotechnology Research Institute

Abstract :

One maglev vehicle is composed of 6 or 8 modules. Each module is composed of 4 staggered magnets attached to an aluminum bogie. In the view point of levitation control except propulsion by LIM, 5 is the maximum degrees of freedom to be controlled. But rolling control of the vehicle depends on the bogie structure. We describe just anti-roll type out of bogie structures and 4 degrees of freedom control is sufficient for levitation quality improvement. Multivariable pole-placement concept and the decentralized control concept are used for controller design. Computer simulation and control experiment are performed on a specially designed test module.

1. Introduction

In most cases, maglev vehicle consists of 6 modules, while each module is composed of 4 magents attached to a rigid body. In many analytical design stage, 4 magnets located at each corner of a flat plate model are used for control of roll, pitch, heave and torsion of the plate and lateral motion is considered separately.[1,2]. But in practical design stage, anti-roll beam structure is used very often. This structure makes each module's motion more free compared with tie-bar structure. As each module can move freely except propulsion and rolling direction, we don't need to model a vehicle with 2 modules, i.e. 8magents. So 4 magnet bar, attached not to 4 corners of a plate but to a rigid bar in a staggered array, is suggested and modelled. In this model, torsion of the bar is not considered. Basic modelling concept is combination of 1) 2-magnets bar for vertical mode control and 2) 2 staggered magnets pair for lateral mode control. As the function of anti-roll beam is to prevent rolling mode, which can't be controlled by a relatively slim bar structure, 4 degrees of freedom controller is designed. This is not the best way but good enough for vehicle control.

Previous modelling techniques on 2 staggered magnet and two magnet bar are shown in reference.[2][3] 4 magnets module is modelled in section2 with simulation results. Through the simulation, it is found that the bigger the momentum inertia is, the bigger the effect of pitching control is. Inertia is highly dependent on the position of secondary suspension. Experimental results on small scale test(module) is given to section 3 and section 4 concludes this paper.

2. 4 magnet module modelling and simulation

2.1 modelling[2][3]

Fig1 shows the 1 module system having 4 degrees of freedom. Equations, (2.1)~(2.4) show the attraction & guidance force for magnet 1,2 and magnet 3,4 each, considered the coupling factors inducing pitching mode and yawing mode. Equations,(2.5)-(2.8) show the relation of voltage and current for 4 magnets.

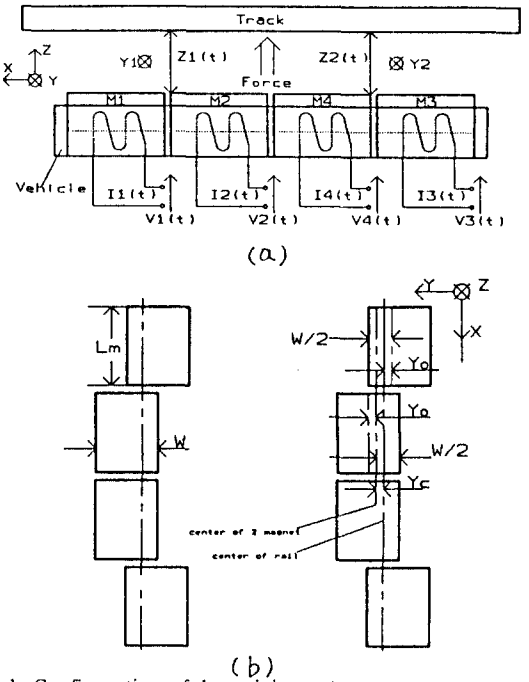

Fig1. Configuration of 1 module system
(a) side view (b) top view

Thus, the basic equation will be derived to analyze the system having the 4 degrees of freedom, as follows.

$$M\frac{d^2z_{m1}}{dt^2}=9.8M-\alpha_{s1}\left[\frac{i_0+i_1}{z_{c1}}\right]^2\cdot\alpha[z_0,y_0+y_{c1}]$$
$$-\alpha_{s1}\left[\frac{i_0+i_2}{z_{c1}}\right]\cdot\alpha[z_0,-y_0+y_{c1}]$$
$$-\alpha_{s2}\left[\frac{i_0+i_3}{z_{c2}}\right]^2\cdot\alpha[z_0,y_0+y_{c2}]-\alpha_{s2}\left[\frac{i_0+i_4}{z_{c2}}\right]^2$$
$$\alpha[z_0,-y_0+y_{c2}]+f_{sdt} \quad \text{----------(2.1)}$$

$$M\frac{d^2y_{m1}}{dt^2}=-\alpha_{s1}\frac{(i_0+i_1)^2}{z_{c1}}\tan^{-1}\frac{y_0+y_{c1}}{z_{c1}}$$
$$-\alpha_{s1}\frac{(i_0+i_2)^2}{z_{c1}}\tan^{-1}\frac{y_0+y_{c1}}{z_{c1}}$$
$$-\alpha_{s2}\frac{(i_0+i_3)^2}{z_{c2}}\tan^{-1}\frac{y_0+y_{c2}}{z_{c2}}$$

$$-\alpha_{g2}\frac{(i_0+i_4)^2}{z_{c2}}\tan^{-1}\frac{y_0+y_{c2}}{z_{c2}}+f_{g0l}\quad\text{----(2.2)}$$

$$M\frac{d^2z_{m2}}{dt^2}=9.8M-\alpha_{s2}\left[\frac{i_0+i_1}{z_{c1}}\right]^2\cdot\alpha[z_0,y_0+y_{c1}]$$

$$-\alpha_{s1}\left[\frac{i_0+i_2}{z_{c1}}\right]\cdot\alpha[z_0,-y_0+y_{c1}]$$

$$-\alpha_{s1}\left[\frac{i_0+i_3}{z_{c2}}\right]^2\cdot\alpha[z_0,y_0+y_{c2}]-\alpha_{s1}\left[\frac{i_0+i_4}{z_{c2}}\right]^2$$

$$\alpha[z_0,-y_0+y_{c2}]+f_{s0l2}\quad\text{----------(2.3)}$$

$$M\frac{d^2y_{m2}}{dt^2}=-\alpha_{g2}\frac{(i_0+i_1)^2}{z_{c1}}\tan^{-1}\frac{y_0+y_{c1}}{z_{c1}}$$

$$-\alpha_{g2}\frac{(i_0+i_2)^2}{z_{c1}}\tan^{-1}\frac{y_0+y_{c1}}{z_{c1}}$$

$$-\alpha_{g1}\frac{(i_0+i_3)^2}{z_{c2}}\tan^{-1}\frac{y_0+y_{c2}}{z_{c2}}$$

$$-\alpha_{g1}\frac{(i_0+i_4)^2}{z_{c2}}\tan^{-1}\frac{y_0+y_{c2}}{z_{c2}}+f_{g0l2}\quad\text{----(2.4)}$$

Where, z1 : vertical air gap of magnet 1,2
y1 : lateral deviation of magnet 1,2
z2 : vertical air gap of magnet 3,4
y2 : lateral deviation of magnet 3,4

$$\alpha_{s1}:\ \frac{\mu_0\cdot lm\cdot w\cdot n^2}{4}\left[-\frac{1}{M}-\frac{1L}{I_p}\right]$$

$$\alpha_{s2}:\ \frac{\mu_0\cdot lm\cdot w\cdot n^2}{4}\left[-\frac{1}{M}+\frac{1L}{I_p}\right]$$

* coupling factor inducing pitching mode.
I_P : pitching inertia

$$\alpha_{g1}:\ \frac{\mu_0\cdot lm\cdot w\cdot n^2}{2\pi}\left[-\frac{1}{M}-\frac{1L}{I_y}\right]$$

$$\alpha_{g2}:\ \frac{\mu_0\cdot lm\cdot w\cdot n^2}{2\pi}\left[-\frac{1}{M}+\frac{1L}{I_y}\right]$$

* coupling factor inducing yawing mode.
I_y : yawing inertia.

l : distance from center of bar to gap sensor

L : distance between center of each magnet

Also, circuit equations for 4 magnet are as follows.

$$e_1=\left|R_a-\frac{z_{c1}L_\beta}{\left[z_{c1}^2+(y_{c1}+y_0)^2\right]^{\frac{3}{2}}}\frac{dz_{c1}}{dt}\right.$$

$$\left.-\frac{(y_{c1}+y_0)\cdot L_\beta}{\left[z_{c1}^2+(y_{c1}+y_0)^2\right]^{\frac{3}{2}}}\cdot\frac{dy_{c1}}{dt}\right|i_1$$

$$+\left|L_{a1}+\frac{L_\beta}{\left[z_{c1}^2+(y_{c1}+y_0)^2\right]^{\frac{1}{2}}}\right|\frac{di_1}{dt}$$

$$-i_0\frac{z_{c1}L_\beta}{\left[z_{c1}^2+(y_{c1}+y_0)^2\right]^{\frac{3}{2}}}\frac{dz_{c1}}{dt}$$

$$-i_0\frac{(y_{c1}+y_0)L_\beta}{\left[z_{c1}^2+(y_{c1}+y_0)^2\right]^{\frac{3}{2}}}\frac{dy_{c1}}{dt}$$

----------(2.5)

$$e_2=\left|R_b-\frac{z_{c1}L_\beta}{\left[z_{c1}^2+(y_{c1}+y_0)^2\right]^{\frac{3}{2}}}\frac{dz_{c1}}{dt}\right.$$

$$\left.-\frac{(y_{c1}-y_0)\cdot L_\beta}{\left[z_{c1}^2+(y_{c1}-y_0)^2\right]^{\frac{3}{2}}}\cdot\frac{dy_{c1}}{dt}\right|i_2$$

$$+\left|L_{a2}+\frac{L_\beta}{\left[z_{c1}^2+(y_{c1}-y_0)^2\right]^{\frac{1}{2}}}\right|\frac{di_2}{dt}$$

$$-i_0\frac{z_{c1}L_\beta}{\left[z_{c1}^2+(y_{c1}-y_0)^2\right]^{\frac{3}{2}}}\frac{dz_{c1}}{dt}$$

$$-i_0\frac{(y_{c1}-y_0)L_\beta}{\left[z_{c1}^2+(y_{c1}-y_0)^2\right]^{\frac{3}{2}}}\frac{dy_{c1}}{dt}$$

-------(2.6)

$$e_3=\left|R_c-\frac{z_{c2}L_\beta}{\left[z_{c2}^2+(y_{c2}+y_0)^2\right]^{\frac{3}{2}}}\frac{dz_{c2}}{dt}\right.$$

$$\left.-\frac{(y_{c2}-y_0)\cdot L_\beta}{\left[z_{c2}^2+(y_{c2}-y_0)^2\right]^{\frac{3}{2}}}\cdot\frac{dy_{c2}}{dt}\right|i_3$$

$$+\left|L_{a3}+\frac{L_\beta}{\left[z_{c2}^2+(y_{c2}-y_0)^2\right]^{\frac{1}{2}}}\right|\frac{di_3}{dt}$$

$$-i_0\frac{z_{c2}L_\beta}{\left[z_{c2}^2+(y_{c2}-y_0)^2\right]^{\frac{3}{2}}}\frac{dz_{c2}}{dt}$$

$$-i_0\frac{(y_{c2}-y_0)L_\beta}{\left[z_{c2}^2+(y_{c2}-y_0)^2\right]^{\frac{3}{2}}}\frac{dy_{c2}}{dt}$$

------(2.7)

$$e_4=\left|R_d-\frac{z_{c2}L_\beta}{\left[z_{c2}^2+(y_{c2}+y_0)^2\right]^{\frac{3}{2}}}\frac{dz_{c2}}{dt}\right.$$

$$\left.-\frac{(i_0+i_2)^2}{(y_{c2}+y_0)\cdot L_\beta}\frac{y_0+y_{c1}}{\left[z_{c2}^2+(y_{c2}+y_0)^2\right]^{\frac{3}{2}}}\cdot\frac{dy_{c2}}{dt}\right|i_4$$

$$+\left|L_{a1}+\frac{L_\beta}{\left[z_{c2}^2+(y_{c2}+y_0)^2\right]^{\frac{1}{2}}}\right|\frac{di_4}{dt}$$

$$-i_0\frac{z_{c2}L_\beta}{\left[z_{c2}^2+(y_{c2}+y_0)^2\right]^{\frac{3}{2}}}\frac{dz_{c2}}{dt}$$

$$-i_0 \frac{(y_{c2}+y_0)L_\phi}{\left\{ z_{c2}^2+(y_{c2}+y_0)^2 \right\}^{\frac{3}{2}}} \frac{dy_{c2}}{dt}$$

--------(2.8)

Also, the linearized model on the equilibrium point (y_0,z_0,i_0), $(-y_0,z_0,i_0)$ by taylor series expansion is given to eqn.(2.9)

$$\dot{x}_1 = A_1X_1 + A_1X_1 + A_{12}X_2 + B_1U_1 + F_{sd1} \quad \text{----(2.9)}$$

$x_1 = [z_1, \dot{z}_1, i_1, y_1, \dot{y}_1, i_2]$;
state variable in magnet 1,2
$x_2 = [z_2, \dot{z}_2, i_3, y_2, \dot{y}_2, i_4]$;
state variable in magnet 3,4

$$u_1 = \begin{bmatrix} e_1 \\ e_2 \end{bmatrix}$$

$$B_1 = \begin{bmatrix} 0 & 0 \\ 0 & 0 \\ \frac{1}{L_{g1}} & 0 \\ 0 & 0 \\ 0 & 0 \\ 0 & \frac{1}{L_{g2}} \end{bmatrix}$$

$$A_1 = \begin{bmatrix} 0 & 1 & 0 & 0 & 0 & 0 \\ \frac{2\beta_s\alpha_s}{M} & 0 & \frac{s}{M} & 0 & 0 & \frac{\beta_s}{M} \\ 0 & \frac{i_0\zeta_s}{L_{s1}} & \frac{R_a}{L_{s1}} & 0 & \frac{i_0\zeta_g}{L_{s1}} & 0 \\ 0 & 0 & 0 & 0 & 1 & 0 \\ 0 & 0 & \frac{\beta_g}{M} & \frac{2\beta_g\zeta_g}{M} & 0 & \frac{\beta_g}{M} \\ 0 & \frac{i_0\zeta_s}{L_{s2}} & 0 & 0 & \frac{i_0\zeta_g}{L_{s2}} & \frac{R_b}{L_{s2}} \end{bmatrix}$$

$$A_{11} = \begin{bmatrix} 0 & 0 & 0 & 0 & 0 & 0 \\ -2\beta_s\alpha_s\beta_1 & 0 & \beta_s\beta_1 & 0 & 0 & \beta_s\beta_1 \\ 0 & 0 & 0 & 0 & 0 & 0 \\ 0 & 0 & 0 & 0 & 0 & 0 \\ 0 & 0 & \beta_g\beta_{y1} & 2\beta_g\zeta_g\beta_{y1} & 0 & -\beta_g\beta_{y1} \\ 0 & 0 & 0 & 0 & 0 & 0 \end{bmatrix}$$

$$A_{12} = \begin{bmatrix} 0 & 0 & 0 & 0 & 0 & 0 \\ -2\beta_s\alpha_s\beta_2 & 0 & -\beta_s\beta_2 & 0 & 0 & \beta_s\beta_2 \\ 0 & 0 & 0 & 0 & 0 & 0 \\ 0 & 0 & 0 & 0 & 0 & 0 \\ 0 & 0 & -\beta_g\beta_{y2} & 2\beta_g\zeta_g\beta_{y2} & 0 & -\beta_g\beta_{y2} \\ 0 & 0 & 0 & 0 & 0 & 0 \end{bmatrix}$$

where

$$\beta_1 = -\frac{l \cdot L}{I_p}$$

$$\beta_2 = -\frac{1}{M} + \frac{l \cdot L}{I_p}$$

$$\beta_{y1} = -\frac{l \cdot L}{I_y}$$

$$\beta_{y2} = -\frac{1}{M} + \frac{l \cdot L}{I_y}$$

If eqn (2.9) is rewritten as general form, it becomes

$$\dot{X}_i = A_iX_i + \Sigma A_{ij}X_j + B_iU_i + D_iTd_i \quad i,j = 1,2 \quad \text{--(2.10)}$$

and it is represented to block diagram in Fig2.

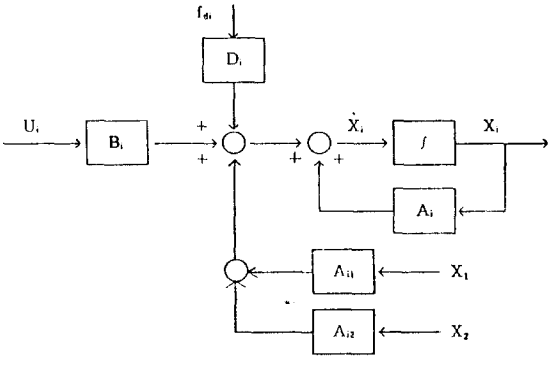

Fig2. Linearized model considering the coupling factor

2.2 Controller design [2]

Pitching and yawing mode may occur to by the coupling factor (A_{i1},A_{i2}) in eqn(2.10). When A_{i1} and A_{i2} are equal to 0, there are the independent two pairs of the staggered magnets. Thus, the guidance and pitching mode can be independently utilized to design the controller of the 4 degrees of freedom. The concept of guidance control can be adopted to the local controller design, and pitching control can be to the global controller design.

Then, $u_i = u_i^l + u_i^g$, $i = 1, 2$ ----------(2.11)

where, u_i : integrated control
u_i^l : local control
u_i^g : global control

Now,let's try to design u_i^l, u_i^g.

First, local control law is to design the levitation and guidance controller for the locally coupled staggered magnets. But there are no interaction between two edges consisted of the staggered two magnets. The locally coupled staggered magnets is represented to 2 input (e_1,e_2)-2 output (z,y) system, and control gain can be obtained by pole placement method.[2]

Next, setting the global control law as eqn(2.12).

$$u_i^g = -\sum_{j=1}^{2} h_{ij}x_j \quad \text{----------(2.12)}$$

The closed-loop system becomes as follows.

$$\dot{x}_i = (A_i - b_i \cdot h_i)x_i + -\sum_{j=1}^{2}(A_{ij} - b_i h_{ij})x_j, i=1,2$$
$$\text{----------(2.13)}$$

The decoupled part of eqn (2.13) can be transformed to quasi-diagonal form to solve the global control law.

Then

$$x_i = T_i \cdot \bar{x}_i \quad \text{----------(2.14)}$$

Where T_i linear nonsingular transformation.

Combining eqn (2.13) with (2.14), eqn (2.13) becomes as follows.

$$\dot{\bar{x}}_i = \Lambda_i \bar{x}_i - \sum_{j=1}^{2}(\bar{a}_{ij} - \bar{b}_i \cdot \bar{h}_{ij})\bar{x}_j, \; i=1,2 \text{--(2.15)}$$

Where, $\Lambda_i = T_i^{-1}(A_{ij} - b_i \cdot h_i)T_i$

$\bar{A}_{ij} = T_i^{-1} A_{ij} T_i$

$\bar{b}_i = T_i^{-1} b_i$

$\bar{h}_{ij} = h_{ij} T_i$ ----------(2.16)

$\bar{h}_{ij}$ becomes by the sevastyano-kotelyanskii's condition to eqn (2.17)

$\bar{h}_{ij} = [(\bar{b}_i^T \cdot \bar{b}_i)^{-1} \cdot \bar{b}_i^T \cdot \bar{A}_{ij}]^T$ ----------(2.17)

and global controller gain, h_{ij} becomes

$h_{ij} = \bar{h}_{ij} \cdot T_i^{-1}$ ----------(2.18)

Now u_i^l and u_i^g is obtained, and the block diagram of total colsed-loop system is given to Fig3. (Decentralized control concept)

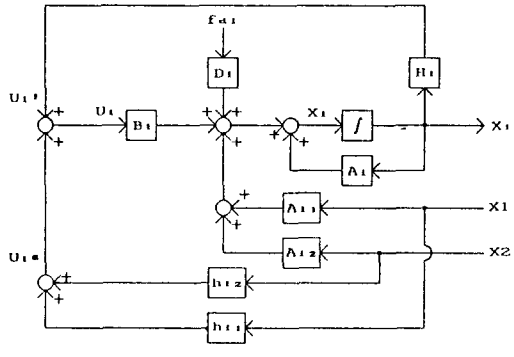

Fig3. Block diagram representing the concept of the integrated control

2.3 Simulation

In this section, the results of computer simulation are shown and explaind. The utilized parameters are as follows.

Total Mass	m = 1874(kg)
Distance between the center of magnet 1,2' mass	L = 1.8(m)
and magnet 3,4'	
Distance between gap and body center	l = 1.8(m)
pitch inertia	I_p = 3800(kg·m^2)
yaw inertia	I_y = 3000(kg·m^2)
nominal inductance	L = 0.31(H)
Resistance	R = 1.344(Ω)
Initial gap	Z_1 = 18(mm)
	Z_2 = 20(mm)
length of magnet	l_m = 841(mm)
width of magnet pole	w_m = 28(mm)
coil turns	N = 480

To calculate the local control gain, the characteristics of closed loop system is determined locally to each of the 2 directions - vertical and lateral direction.

For most full scale magnetically suspended vehicles, the natural frequency is in the 4~10 Hz range [2,3]. Here 6Hz is chosen. Also, the damping ratio with which ride quality is concerned is 0.707 for suspansion control. 3Hz(natural frequency) and 0.25 (damping ratio) is chosen for guidance control. And real pole value is chosen -45 for both. With these values the control gain are obtained, and it is shown below.

H =

$$\begin{bmatrix} 89114.5 & 2438.1 & -23.8 & 38258.9 & 1644.9 & -8.25 \\ 89114.5 & 2438.1 & -8.25 & -38258.9 & -1644.9 & -23.8 \end{bmatrix}$$

Also, utilizing the method referred to chap2, the global gain can be obtained and it is shown, too.

H_{11} =

$$\begin{bmatrix} 16978.3 & 0 & -1.86 & 10886.8 & 0 & -7.0 \\ 16978.3 & 0 & -7.0 & -10886.8 & 0 & 1.86 \end{bmatrix}$$

H_{12} =

$$\begin{bmatrix} -6232.55 & 0 & -0.36 & -5371.5 & 0 & -2.9 \\ -6232.55 & 0 & -2.9 & 5371.5 & 0 & -0.36 \end{bmatrix}$$

Fig4 shows the vertial(z_1,z_2) and lateral(y_1,y_2) gap, in the local suspension control without guidance.

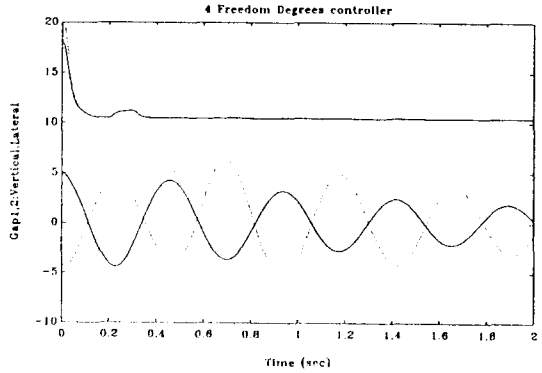

Fig4. Signals in the local suspension control without guidance control

Fig5 shows the same signal as Fig4 in the local suspension except performing guidance control.

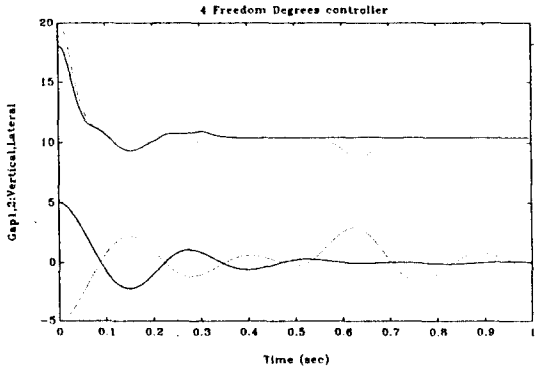

Fig5. Local suspension control with guidance control (comparing Fig4)

The initial vertial gap is set to z_1=18, z_2=20[mm], and lateral deviation is y_1=5 and y_2=-5[mm], too.

Also, the vertical disturbance which is 20% of total mass is given between 0.2 sec and 0.3 sec. And the lateral disturbance which is 5% of total mass is between 0.5 and 0.6 sec.

Comparing 2 figures, both figures are almost similar in pitching mode for the vertical disturbance, but it is shown that Fig4 (only suspension control) is better in pitching mode for the lateral distarbance.

However, it also has the difficulty in damping the lateral fluctuation.

Fig6 shows the pitch angle and pitch velocity in case of Fig5.

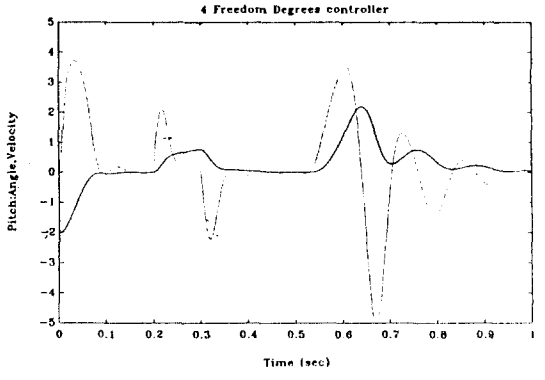

Fig6. Pitch angle and pitch velocity in case of Fig5

Fig7 shows the response in controlling 4 degrees of freedom.

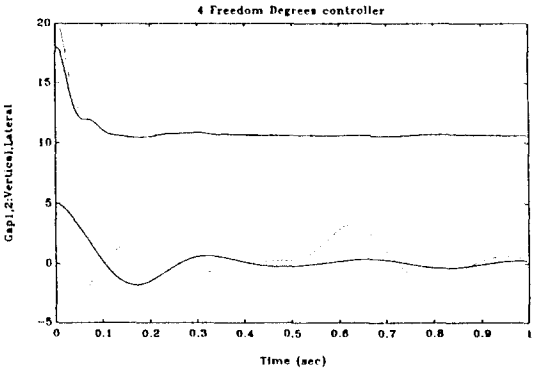

Fig7. Signals in the integrated control

Fig8 shows pitch angle and pitch velocity in case of Fig7.

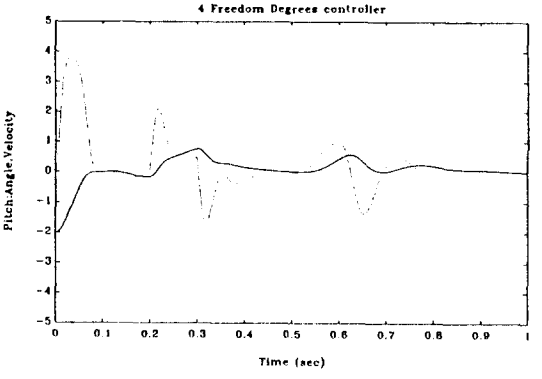

Fig8. Pitch angle and pitch velocity in case of Fig7

Comparing Fig6 with Fig8, it is knowns that the control of 4 freedom degrees shows the better response against vertical and lateral disturbances.

3. Experimental results

3.1 One module test jig

First, the experimental apparatus are briefly mentioned. The supply voltage in magnet is 100 V D.C source to which A.C voltage is rectified by diode full bridge method. And chopping frequency is 2 KHz. Active analog filter is utilized to filter the sensor signals. Also, 16 bit-μ processor (8797) is used to calculate the control input. The special plant to control 4 freedom digrees has been built and it has 2 linear guide, 1 ball-bush shaft, and 1 support bearing in addition to the part to insert the disturbances.

3.2 Results

Fig9 shows the lateral gap, the pitching angle and vertical gap, from top.

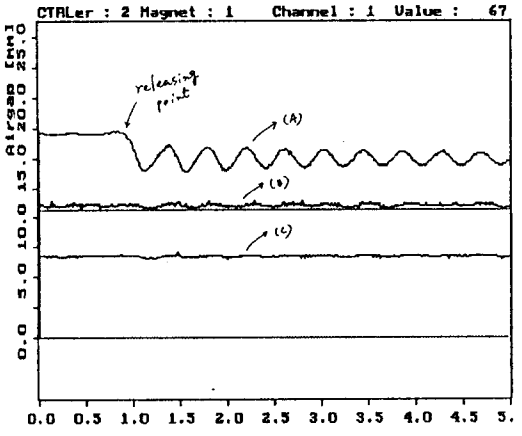

Fig9. Experiment signals in the local control without guidance control

Briefly metioning the experiment method, after the suspension ended completely, i.e. plant was located at steady state, plant was drawn to the diagonal direction(45°) with the about 5% force of plant weight.

In a moment, at a releasing point the plant was released. Then the signals were catched for some time. Fig10 shows the obtained signal in the global control without guidance control.

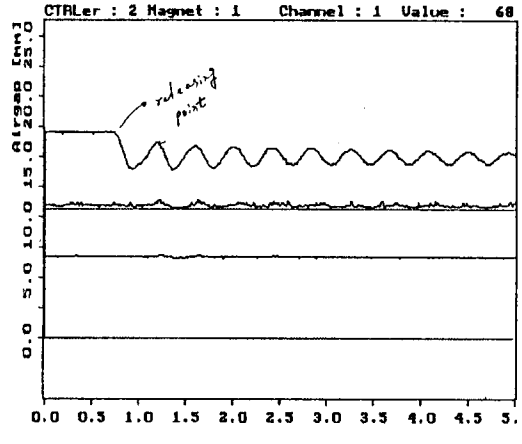

Fig10. Global suspension control without guidance control (compare Fig9)

Fig11 shows the obtained signal in controlling the 4 freedom degrees.

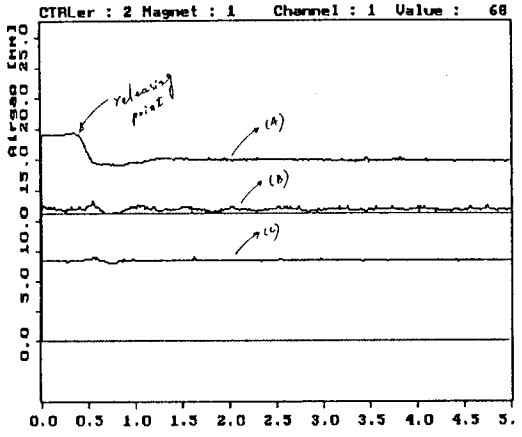

Fig11. Signals in controlling the 4 freedom degrees

This result coincides with the simulation result very well.

Comparing these figures, it is shown that the response characteristics of vertical and lateral directions are ameliorated through the control of 4 freedom degrees.

4. Conclusion

In this paper, the integrated concept to control the 4 degrees of freedom was introduced for one module.

The controller of 4 degrees of freedom shows the better response than edge controller(not to consider the coupling factor) through computer simulation and experiment. And this results will be easily adopted to the practical vehicle.

5. Reference

1. Sinha, "Electromagnetic Suspension Dynamics & Control", 1987

2. KERI report, " A study on development of technologies for magnetic levitation and propulsion system", 1991.9, 1993.3

3. 勘西一, "電磁吸引式 磁氣浮上車兩の左右案內制御", 1989

4. J.M.Maciejowski, "Multivariable Feedback Design", 1989

5. Cleve Moler, "PC-MATLAB for MS-DOS personal computer", 1987